

Enthalpy and entropy of twin boundaries in superconducting $\text{YBa}_2\text{Cu}_3\text{O}_{7-x}$

Linfeng Mei^{a)} and Siu-Wai Chan^{b)}

Department of Applied Physics and Applied Mathematics, Columbia University, New York, New York 10027

(Received 24 November 2004; accepted 16 June 2005; published online 9 August 2005)

Twin boundary energy (γ_{tw}) and its temperature dependence are important factors to be evaluated for engineering twin morphology for strong flux pinning and high critical current density in superconducting $\text{YBa}_2\text{Cu}_3\text{O}_{7-x}$. Here, it has been measured as a function of oxygenation temperature from 450 to 680 °C using both the twin spacing method and a twin tip method. By comparing the twin energies obtained by the two methods, the geometrical factor α used in twin spacing method is determined. This geometrical factor is directly related to the sharpness of the twin tips. From the temperature dependence of twin boundary energy per unit area, twin boundary entropy (Δs) and enthalpy (Δh) for twin boundaries are projected to be 0.24 mJ/K m² and 246 mJ/m², respectively. © 2005 American Institute of Physics. [DOI: 10.1063/1.1999034]

I. INTRODUCTION

Twin engineering by increasing the oxygenation temperature can result in narrow twin spacings, a concomitant high critical current density (J_c) and a strong flux-pinning force (F_p) in melt-textured-grown (MTG) Y–Ba–Cu–O (YBCO) superconductor. Hence, twin refinement in YBCO is of technological importance for wire and tape developments. Twin refinement using higher oxygenation temperatures is based on the premise that the twin boundary energy of $\text{YBa}_2\text{Cu}_3\text{O}_{7-x}$ (Y123) decreases with increasing oxygenation temperature due to a positive entropy. Twin boundary energy (γ_{tw}) is an important parameter to master for engineering twin microstructure for strong flux pinning and high critical current density in YBCO. Here, we show how it can be changed by changing the oxygenation temperature and be measured by both the traditional twin spacing method and a twin tip method.

II. BACKGROUND AND THE TWIN SPACING METHOD

The principle of the twin spacing method is that an average twin spacing is a result of energy minimization in the twin colony, while a twin colony can be defined as a region of parallel twins that are bounded in the same direction. In polycrystalline Y123, the size of a twin colony is usually, though not always, equal to the grain size. In a MTG YBCO pellet which is a single grain of Y123 with finely dispersed Y_2BaCuO_5 (211) particles, the twin colony sizes are much smaller than “the grain size of Y123” and usually of the order of the 211 interparticle spacings.¹ As found in other twinned materials, individual twins in YBCO are lenticular in shape. A twin is composed of both coherent and incoherent twin boundary segments. The different segments will have different boundary energies. The coherent segment usually dominates the flat and smooth parts of the twin and short incoherent segments separated by long coherent segments are at the advancing tips. The sharper the tips, the more

predominate are the coherent segments at the tips. Therefore, the twin boundary energy determined below is closely representing the coherent twin boundary energy. The total energy of a twin colony includes both its area sum of the twin boundary energy (E_{twin}) and the associated elastic strain energy (E_{strain}) located around individual twin tips. Shown in Fig. 1, the problem is reduced into two dimensions with a twin colony of a twin spacing of T_w , with average twin thickness of t_w ($t_w \approx T_w$), twin colony length $L_1 = 2L$, width L_2 , and thickness L_3 . Individual twin length is $2L$, and the coordinate along the twin length is x with $x=0$ at the center of the twin and $x=L$ at the tip of the twin. The profile of a twin is expressed as $h(x)$ with $h(0) = \frac{1}{2}T_w$ and $h(L) = 0$. The shear strain (ε) that accompanied the tetragonal-to-orthorhombic (T -to- O) transformation is

$$\varepsilon = 2(b_0 - a_0)/(b_0 + a_0) \approx b_0/a_0 - 1, \quad (1)$$

where a_0 and b_0 are the lattice parameters along x and y axes, respectively. ε is also known as the orthorhombicity of Y123, and

$$b_0/a_0 = \tan[(\pi/4) + (\phi/4)]. \quad (2)$$

The angle ϕ can be measured from the $(1\bar{1}0)$ spot splitting on the (001) selected area diffraction pattern (SADP). If the strain for an individual twin is assumed to be confined within the small regions at the two lenticular edges, each small re-

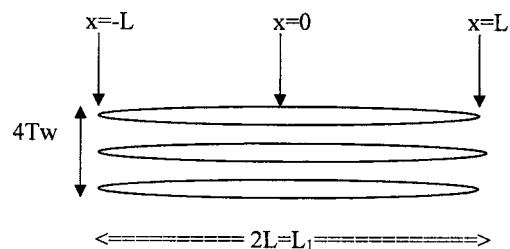


FIG. 1. A schematic diagram showing a twin colony with a set of parallel twins. Only three twins are shown here. Usually, there are 10–20 twins. The coordinate along the twin length is x , where $x=0$ at the twin middle or root and $x=L, -L$ at the twin tips. The profile of a twin is $h(x)$. $T_w = t_w = 2h(0)$ is the twin thickness.

^{a)}Present address: 5863 Rue Ferrari, Western Digital Corporation, San Jose, CA 95138.

^{b)}Electronic mail: SC174@columbia.edu

gion has a characteristic length scale of twin spacing (T_w), then the total energy can be expressed as

$$E_{\text{total}} = E_{\text{twin}} + E_{\text{strain}} = \gamma L_1 L_3 (L_2/T_w) + 0.5 \mu \varepsilon^2 (T_w)^2 L_3 (L_2/T_w). \quad (3)$$

Taking the derivative with respect to T_w and setting the derivative to zero for energy minimization, we obtain

$$T_w = \sqrt{\gamma_{\text{tw}} L_1 / 0.5 \mu \varepsilon^2} \quad (4)$$

or generally

$$T_w = \sqrt{\gamma_{\text{tw}} G / \alpha \mu \varepsilon^2}, \quad (5)$$

where G is the twin colony size, μ is the shear modulus, α is the geometrical factor in place of 0.5, and γ_{tw} is the twin boundary energy per unit area. For twinning dislocations of the edge type, Eq. (5) needs to be modified to

$$T_w = \sqrt{(1-\nu) \gamma_{\text{tw}} G / \alpha \mu \varepsilon^2}. \quad (6)$$

Similar equations have been derived by Arlt *et al.*,² Chumbley *et al.*,³ Roy and Mitchell,⁴ and Muller and Freyhardt.⁵ The conclusion drawn from the energy minimization is that twin spacing is proportional to the square root of the colony size G . With the measured twin spacing T_w and twin colony size G from microscopy, the twin boundary energy γ_{tw} can be obtained from Eq. (5) and (6). More accurately one can determine the best value of twin boundary energy (γ_{tw}) from the slope of the best-fitted straight line of the data of twin spacing versus (colony size)^{1/2}.

It should be pointed out that different estimates of the strain volume around the tip of a twin (i.e., different α values) will yield different values of the twin boundary energy γ_{tw} . The following are some remarks for the above equations.

- (1) In Eq. (4), a geometrical factor $\alpha=0.5$ is used, which means that the region under elastic strain only extends to T_w from the twin tip. The individual strain region and E_{strain} will be larger if a larger α value is needed which indicates shaper twin tips.
- (2) In practice, twins in YBCO [as observed by transmission electron microscopy (TEM)] consist of edge twinning dislocations rather than screw dislocations.⁶ Therefore, μ should be replaced by $\mu/(1-\nu)$. For Y123, ν is typi-

TABLE I. The reported twin boundary energies γ_{tw} 's in Y123.

| γ_{tw} (mJ/m ²) | Method | Ref. |
|---|---|------|
| 0.1 | Measurement of T_w in lamellae | 3 |
| 2.8 | Ditto | 4 |
| 8.5 (upper limit) | Ditto | 5 |
| 2.6 (lower limit) | Ditto | 5 |
| 80 | Ditto | 7 |
| <40 | Coercive stress (25 MPa) and T_w | 8 |
| 1000 | Measurement of h/l ratio | 9 |
| 28.9 (without PtO ₂), | Measurement of T_w in lamellae, S_{211} was used instead of G | 10 |
| 11.35 (with PtO ₂) | Ditto | 10 |

cally 1/3–1/4, which results in an increase of 1/3–1/2 in E_{strain} with corresponding increases in γ_{tw} .

- (3) The equations require that the twin colony size is much greater than the pileup length at twin tip and are only applicable to narrowly spaced twins.

As shown in Table I, the twin boundary energy (γ_{tw}) of Y123 determined by the twin spacing method was reported to be 0.1 mJ/m² by Chumbley *et al.*,³ 2.8 mJ/m² by Roy and Mitchell,⁴ 2.6–8.5 mJ/m² by Muller and Freyhardt,⁵ and 80 mJ/m² by Zhu *et al.*⁷ While considering the energy balance between the twin boundary energy and the work done by the coercive stress during the introduction of twin variant, LaGraff and Payne⁸ evaluated the upper limit of γ_{tw} in Y123 as 40 mJ/m². Boyko *et al.*⁹ used the experimental thickness h and length L of wedge-shaped twins, and estimated γ_{tw} to be 1000 mJ/m².

The reported values of the twin boundary energy (γ_{tw}) span over four orders of magnitudes (i.e., from 0.1 to 1000 mJ/m²), and yet no temperature-dependent twin boundary energy of Y123 has been reported. The big differences in the reported twin boundary energy warrant further investigation. We will first reexamine the twin spacing method. Among the parameters used for determining γ_{tw} , the geometric factor α has taken values of 1, 0.5, 0.32, and even 0.002 488 (i.e., a factor of 400 in variation), while the shear modulus or C_{66} the stiffness constant has been taken from 59 to 200 GPa (i.e., a factor of 3.4), and the shear strain ε from 0.0145 to 0.018, with ε^2 varying by 1.54 times. The differences in the reported γ_{tw} values by different groups are likely

TABLE II. Summary of the reported values of Young's modulus (E), stiffness constants (C_{xx} 's), shear modulus (μ), Poisson's ratio (ν) of Y123, and the measuring methods used.

| Sample type | Measurement method | E, C_{xx} (GPa) | μ, C_{66} (GPa) | ν | Ref. |
|----------------|----------------------------------|---|---------------------|-------|------|
| Single crystal | Brillouin Spectroscopy | $C_{11}=211; C_{33}=159; C_{44}=33$ | NA | NA | 11 |
| Polycrystals | Nanoindentation | 154.3 | NA | NA | 12 |
| Polycrystals | Pulse-echo | 148.1 | 59 | | 13 |
| Single crystal | Inelastic neutron scattering | $C_{11}=C_{22}=230; C_{33}=150; C_{44}=C_{55}=50$ | $C_{66}=85$ | NA | 14 |
| Single crystal | Estimate | 151 | $59, C_{66}=97$ | 0.281 | 15 |
| Single crystal | Sound velocity | $C_{33}=160$ | $C_{66}=82$ | NA | 16 |
| Polycrystals | Ultrasonic pulse-echo | 180 (estimate) 126 (90% dense) | NA | NA | 17 |
| Single crystal | Resonant ultrasound spectroscopy | 154.3 | $C_{66}=95$ | 0.314 | 18 |
| Single crystal | Estimate | 159.3 | 61.48 | 0.295 | 19 |

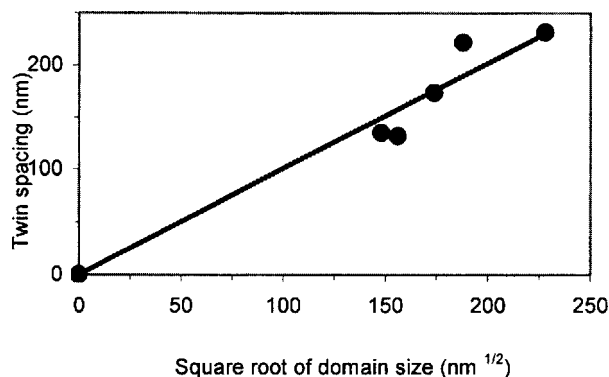


FIG. 2. The twin spacing (T_w) vs square root of domain size ($G^{1/2}$) for sample 450.

due to these different parameters used. If the reported γ_{tw} values are normalized with the same set of α , C_{66} , and ε^2 then the comparison based on the "normalized" γ_{tw} 's will show whether the differences in the reported γ_{tw} 's are intrinsic. The reported Young modulus ($E=150\text{--}160$ GPa), shear modulus (μ), Poisson's ratio ($\nu=0.3$) of Y123, and the measurement methods used are listed in Table II. The stiffness constant $C_{66}=95$ GPa is used rather than the polycrystalline shear modulus $\mu=59$ GPa since twinning involves shear in the (001) plane of Y123. The normalized γ_{tw} 's, with $\alpha=0.5$, $C_{66}=95$ GPa, and $\nu=0.3$, are in the range from 2 to 30 mJ/m² when determined by the twin spacing method. The twin boundary energy evaluated using the coercive stress and twin spacing⁸ is not exact because the method only gives the upper limit of γ_{tw} and it depends strongly on the coercive stress which is hard to determine precisely. The highest reported γ_{tw} (1000 mJ/m²) was obtained by Boyko *et al.*⁹ by a twin shape method. In their method, the twin boundary was described as a stacked array of pileup dislocations. There are mistakes in their assumption and definition which we will discuss later. The energy of a coherent twin boundary in a metal is typically around 5% of the energy of a random high-angle grain boundary.^{20–22} For Y123, the high-angle grain-boundary energy is about 800 mJ/m²,²³ which gives an estimate of the twin boundary energy of 40 mJ/m².

Twin boundary energy (γ_{tw}) of Y123 is a function of oxygenation temperature, oxygen partial pressure during oxygenation, and its dopants.²⁴ Although γ_{tw} is not dependent on the amount of 211, in an earlier study a high initial 211 vol % (>30 %) in MTG pellets leads to small interparticle distances which restrict twin colony size and thus refine twin spacing.²⁵ It has been reported that PtO₂ doping can reduce twin boundary energy of Y123 by 60%. Chopra *et al.*, Chen *et al.*, and Boyko *et al.* found that PtO₂-doped Y123 has a γ_{tw} of 18.28 mJ/m² which is lower than 46.53 mJ/m² for YBCO without PtO₂ doping.^{10,25} Here, all the samples used for γ_{tw} measurement have the same initial 211 volume of 28.6%, and are all PtO₂ doped and prepared under the same MTG conditions, such that γ_{tw} can be studied as a function of oxygenation temperature alone. All present annealing is performed under 1 atm of oxygen pressure to maintain the same final oxygen content, since different oxygen partial pressure can change the Y123 oxygen content.

III. EXPERIMENT

All the initial MTG pellets have the same composition which is Y123 with 40-wt % excess 211, 0.5-wt % PtO₂ or also denoted as 28.6-wt % 211, and 71.4-wt % YBCO with 0.5-wt % PtO₂. All pellets are prepared with the same MTG procedure. The samples used are cleaved from the same region of the pellets which are directly under the seed with a size around $3 \times 3 \times 0.5$ mm³ and isothermally annealed at 450, 500, 600, 650, and 680 °C, which is similar to the procedure used by Shaw *et al.*²⁶ Twin boundary energies at different annealing temperatures will be determined by plotting corresponding twin spacing T_w against $G^{1/2}$, where G is the colony size and calculated from the slope of the best-fitting line through Eq. (6). Since the twin spacing in Y123 is in the order of 1000 Å, only TEM can be used to measure both G and T_w accurately. Here, the twin shape as well as both G and T_w is obtained by TEM with beam along the [001] direction. The colony size of parallel twins in the same $\langle 110 \rangle$ variant is evaluated, and the average twin spacing T_w within the colony is measured from TEM micrographs. The colony size G is evaluated by moving the sample to capture different regions on the TEM screen from one edge of the colony to the other. Different microfeatures including 211 particles are used as markers to collage different micrographs in order to measure the colony size G . Since the colony sizes are quite large in these samples, only a few colonies are within the electron transparent area in each TEM sample. Since twin spacings within one colony are nonuniform, the average twin spacing T_w is determined by taking many TEM micrographs for one colony. The orthorhombicity ε can be confirmed from the (1 $\bar{1}$ 0) spot splitting on (001) SADP. The error in our T_w measurement is about 10%, with the corresponding error in the γ_{tw} value being 20% as measured by the twin spacing method.

Figure 2 is the plot of twin spacing versus the square root of colony size (i.e., T_w vs $G^{1/2}$ for the sample annealed at 450 °C for 30 h also referred as sample 450. The through-zero-linear-fit line has a slope of 1.006 (nm)^{1/2}. As mentioned, twins are viewed along the [001] direction showing twin dislocations as edge type,^{7,10} this means that Eq. (6) should be used instead of Eq. (5). Using $\alpha=0.5$, $C_{66}=95$ GPa, $\varepsilon=0.0171$, and $\nu=0.3$, the twin boundary energy of Y123 at 450 °C, $\gamma_{tw,450\text{ }^\circ\text{C}}$, is calculated as 20.1 mJ/m². Similarly in Fig. 3, there is also a linear relation between the twin spacing and the square root of the colony size for sample 500. A through-zero linear fit yields a slope of 0.8697 (nm)^{1/2}. Using this slope and ε of 0.0169, the twin boundary energy of Y123 at 500 °C, $\gamma_{tw,500\text{ }^\circ\text{C}}$, is computed to be 15.6 mJ/m². The slope of T_w vs $G^{1/2}$ for sample 600 is 0.7663 (nm)^{1/2}, and the twin boundary energy of YBCO at 600 °C, $\gamma_{tw,600\text{ }^\circ\text{C}}$, is computed to be 10.9 mJ/m². Correspondingly, $\gamma_{tw,650\text{ }^\circ\text{C}}$ is 6.6 mJ/m², and $\gamma_{tw,680\text{ }^\circ\text{C}}$ is 3.7 mJ/m². In summary, the γ_{tw} values measured by the twin spacing method are 20.1, 15.6, 10.9, 6.6, and 3.7 mJ/m² for 450, 500, 600, 650 and 680 °C, respectively. From these values of γ_{tw} using the twin spacing method, the twin boundary energy decreases with increasing temperature (Fig. 4).

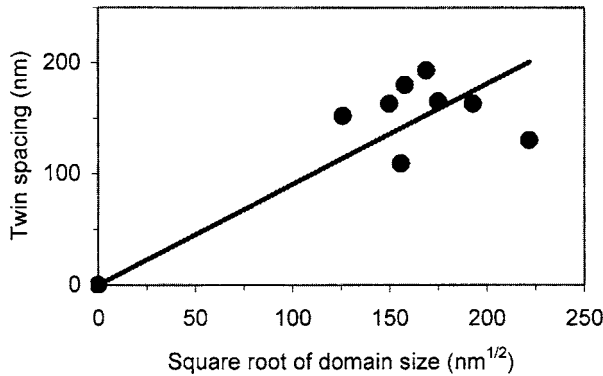


FIG. 3. The twin spacing (T_w) vs square root of domain size ($G^{1/2}$) for sample 500.

IV. BACKGROUND OF THE TWIN TIP METHOD

In the twin spacing method, there is a geometrical factor, α with assigned values from 0.002 488 to 1. Although the relative values of γ_{tw} can be determined by using the same α value, accurate values of γ_{tw} cannot be obtained by the twin spacing method unless α is known. The determination of α involves knowing the strain volume at the twin tip and is intrinsically associated with the tip shape of the twins. Ideally, α can be determined using a careful estimation of this strain volume from the tip shape. Alternatively, the twin tip method can be used to determine the α value. The main ideas behind the twin tip method are the following: a twin can be modeled as a planar pileup of twinning dislocations, and the distribution of the twinning dislocations can be described by a continuous dislocation density function which completely defines the profile $h(x)$ of a twin.²⁵ This method is valid for a thin twin which has a twin thickness [i.e., $t_w = 2h(0)$] much smaller than the twin length L , where $L = L_1/2$ and $h(L) = 0$. Referring to Fig. 1, at a twin tip $x = L$ and $x = 0$ at the middle of the twin. According to this thin twin model, only three parts of a twin have equations that can describe their profiles: the twin tip including the region adjacent to the tip, the intermediate region, and the twin root (i.e., middle). These three different parts of the twin have different dislocation density functions that are well defined. Here we use the twin tip part where the starting point is unambiguous.

Since the twinning dislocations are edge type, the twin boundary energy can be determined by the following set of equations:²⁵

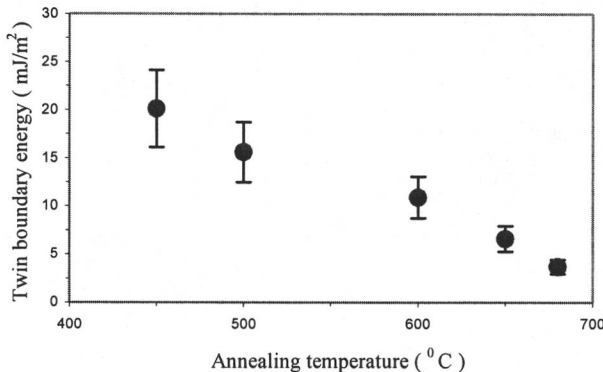


FIG. 4. Temperature dependence of the twin boundary energy calculated by the twin spacing method.

$$\gamma_{tw} \approx \frac{\pi(1-\nu)M^2}{\mu}, \quad (7)$$

where μ is the shear modulus of Y123, ν is the Poisson's ratio, and M is a parameter defined as

$$M = \frac{\sqrt{2}}{\pi} \int_0^L \frac{S_{st}(x)dx}{\sqrt{L-x}}, \quad (8)$$

where $S_{st}(x)$ is the surface-tension stress. For each twin tip, M is constant because S_{st} is zero except for a small region near the twin tip. After some mathematical processing,²⁵ the above equation can be simplified as

$$M = \frac{\mu b \sqrt{L}}{4a(1-\nu)} S_1, \quad (9)$$

where L is the twin length, b is the Burgers vector, and a is the distance between the adjacent gliding planes of twinning dislocations. S_1 is the slope of the linear fit of the plot of $h(x)$ vs $\sqrt{L^2-x^2}$ for the twin tip region. For all calculations by the twin shape method, values of $\mu = C_{66} = 95$ GPa, $\nu \approx 0.3$, $a = 2.7 \times 10^{-10}$ m and $b = 0.85 \times 10^{-11}$ m are used.²⁷ Therefore, γ_{tw} can be determined by the following:

$$\gamma_{tw} = \frac{\pi b^2 L \mu}{16a^2(1-\nu)} (S_1)^2 = 2.76 \times 10^7 L (S_1)^2. \quad (10)$$

For the samples annealed at different temperatures, the twin shape images are taken and digitized by the program NXSCAN.²⁸ The profile and the coordinate $h(x)$ and x are measured for each twin tip. Slopes of $h(x)$ vs $\sqrt{L^2-x^2}$ are found from the corresponding plots. Equations (9) and (10) are applied to determine twin boundary energy. Here the accuracy of γ_{tw} depends strongly on the accuracy of the slope of the linear fit of $h(x)$ vs $\sqrt{L^2-x^2}$ plot. Enlarging the TEM micrograph of the twin tip to obtain accurate $h(x)$ and x coordinates is essential for an accurate value of the slope.

A. Influence of obstacle proximity on the twin tip method

Twin tips from samples 600, 650, and 680 are shown in Figs. 5(a)–5(d). Tables III and IV summarize the results for samples 600 and 650, where the twin energy obtained from twin tips with small d/T_w ratio (d is the distance from the twin tip to the second twin variant) is much larger than those with large d/T_w ratio. In order to know whether the high value of γ_{tw} from tips with small d/T_w ratio is incidental, twin tips in three different samples which are processed and annealed under the same conditions are used to calculate $\gamma_{tw,650^\circ\text{C}}$. The obtained $\gamma_{tw,650^\circ\text{C}}$'s are 84.4, 88.6, and 87.7 mJ/m² for samples 650 (a), 650 (b) and 650 (c), with their corresponding $M_{650^\circ\text{C}}$'s being 4.2×10^4 , 4.3×10^4 , and 4.3×10^4 N/m^{3/2}, respectively. The results are consistent even there are differences in the twin thickness [i.e., T_w or $h(0)$] and the ratio of $h(0)/L$ among the three samples. The high tabulated values of γ_{tw} 's from tips with small d/T_w ratio are not incidental but reflections of strain interaction.

The distance from the twin tip to its neighboring twin variant has a strong effect on the boundary energy determination because when the strain field of an advancing twin tip

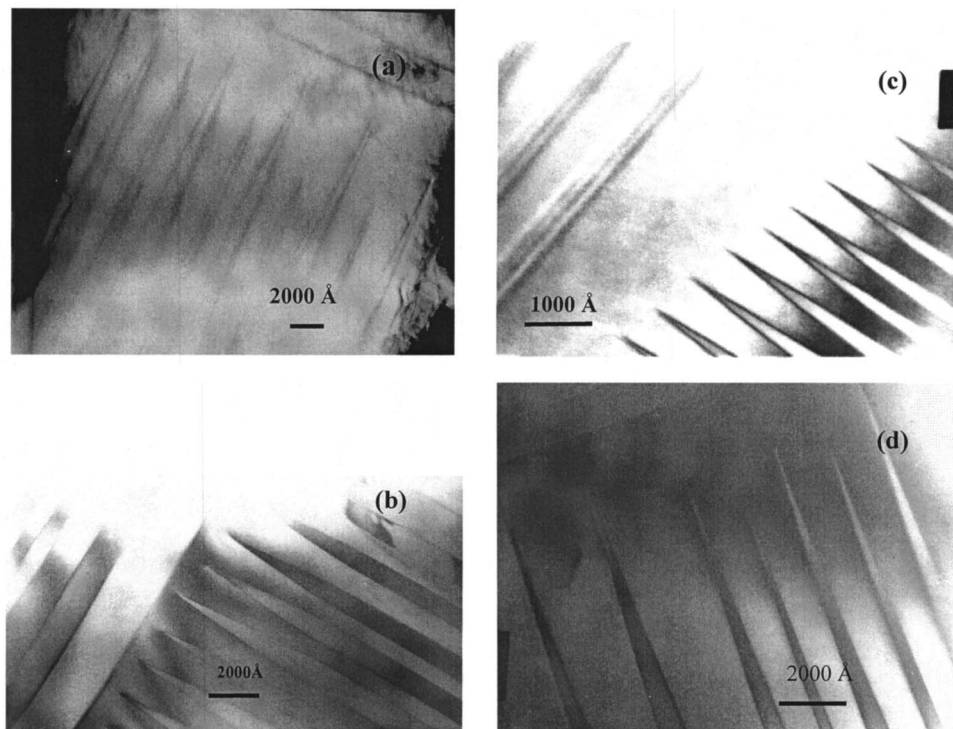


FIG. 5. (a) TEM micrograph showing a set of twin tips in sample 600. (b) TEM micrograph showing a set of twin tips in sample 650 meeting the other twin variant with small obstacle separation, i.e., small d/T_w ratio. (c) TEM micrograph showing a set of twin tips in sample 650 approaching the other twin variant with large d/T_w ratio. (d) TEM micrograph showing a set of twin tips in sample 680 approaching the other twin variant with small d/T_w ratio.

encounters an obstacle, the tip is effectively blunted, giving a seemingly large twin boundary energy under the assumption of free twin tips. Here, the obstacle of advancing twins is the perpendicular twins of the neighboring second variant. The ratio between the distance from a twin tip to an obstacle (d) and the twin thickness (T_w) is used to index the elastic interaction between the tip and the obstacle. As to the temperature effect, assuming that the lattice frictional force acting on the twinning dislocations decreases with increasing temperature, the possibility of a twin to meet the obstacle will increase. At the same time, it is also easier for the tips to contract and change shape due to the high mobility of twinning dislocations. To assess the obstacle effect, twin energies calculated from tips with different d/T_w ratios are compared. The results are listed in Tables III and IV and shown in Figs. 6(a)–6(c).

From Table III for tips with $d/T_w < 5$ (tips 1–5), the average values are $\gamma = 89 \text{ mJ/m}^2$ and $M = 4.3 \times 10^4 \text{ N/m}^{3/2}$, while the averages for tips with $5 < d/T_w < 15$ (tip 6–10), are $\gamma = 32 \text{ mJ/m}^2$ and $M = 2.56 \times 10^4 \text{ N/m}^{3/2}$. The possible free tips (tips 11–14) give $\gamma = 26.7 \text{ mJ/m}^2$ and $M = 2.3 \times 10^4 \text{ N/m}^{3/2}$. When the twin tip is very close to the second twin variant (obstacle), with d/T_w smaller than 5 for sample 600, the twin shape can be significantly changed by the second twin variant. With these blunted tips, the twin boundary energy calculated by the twin tip method will be three to four times as that calculated with free twin tips. Similar phenomena are observed for samples 650 and 680. Theoretically, free twin tips with infinite d/T_w are ideal for twin energy determination using the twin tip method. In practice, if the ratio d/T_w is large enough, γ_{tw} will gradually assume a constant value even with increasing d/T_w ratio, as shown in Figs. 6(a)

TABLE III. The influence of the distance (d) from twin tip to the second twin variant on the twin boundary energy calculation for the samples annealed at 600 °C.

| No. ^a | $h(0)/L$ | $L(10^{-7} \text{ m})$ | Slope | $\gamma(\text{mJ/m}^2)$ | $M(10^4 \text{ N/m}^{3/2})$ | d/T_w |
|------------------|----------|------------------------|----------|-------------------------|-----------------------------|------------------|
| 1 | 0.093 | 12.39 | 0.056 04 | 107.4 | 4.73 | 1.2 |
| 2 | 0.103 | 12.73 | 0.051 | 91.5 | 4.36 | 0.3 |
| 3 | 0.096 | 10.97 | 0.051 14 | 78.7 | 4.06 | 1.8 |
| 4 | 0.098 | 12.16 | 0.050 29 | 84.8 | 4.20 | 1.2 |
| 5 | 0.103 | 11.42 | 0.050 78 | 81.3 | 4.12 | 1.1 |
| 6 | 0.1 | 5.51 | 0.046 34 | 32.7 | 2.61 | 5 |
| 7 | 0.058 | 5.43 | 0.047 84 | 34.3 | 2.67 | 14 |
| 8 | 0.054 | 6.76 | 0.039 48 | 29.1 | 2.46 | 11 |
| 9 | 0.062 | 7.53 | 0.043 65 | 39.6 | 2.88 | 5 |
| 10 | 0.048 | 6.31 | 0.036 63 | 23.4 | 2.21 | 15 |
| 11 | 0.071 | 4.33 | 0.039 03 | 18.2 | 1.95 | Possible freetip |
| 12 | 0.089 | 4.15 | 0.047 86 | 26.2 | 2.33 | Possible freetip |
| 13 | 0.096 | 9.04 | 0.031 44 | 24.6 | 2.27 | Possible freetip |
| 14 | 0.125 | 6.42 | 0.046 04 | 37.5 | 2.80 | Possible freetip |

^aNo. 11–14 are possible free tips.

TABLE IV. The influence of the distance (d) from twin tip to the second twin variant on the twin boundary energy calculation for the samples annealed at 650 °C.

| No. | $h(0)/L$ | $L(10^{-7} \text{ m})$ | Slope | $\gamma(\text{mJ/m}^2)$ | $M(10^4 \text{ N/m}^{3/2})$ | d/T_w |
|-----|----------|------------------------|----------|-------------------------|-----------------------------|---------|
| 1 | 0.126 | 2.44 | 0.063 56 | 27.21 | 2.38 | 4.84 |
| 2 | 0.115 | 2.65 | 0.065 11 | 31.01 | 2.54 | 5.38 |
| 3 | 0.109 | 2.6 | 0.067 89 | 33.07 | 2.63 | 6.33 |
| 4 | 0.115 | 2.45 | 0.066 41 | 29.82 | 2.49 | 6.85 |
| 5 | 0.105 | 2.48 | 0.063 98 | 28.02 | 2.42 | 8.24 |
| 6 | 0.081 | 2.37 | 0.053 85 | 18.97 | 1.99 | 11.69 |
| 7 | 0.106 | 1.97 | 0.068 55 | 25.55 | 2.31 | 11.02 |
| 8 | 0.099 | 1.97 | 0.063 72 | 22.08 | 2.15 | 12.2 |
| 9 | 0.087 | 1.91 | 0.066 64 | 23.41 | 2.21 | 15.9 |
| 10 | 0.102 | 1.81 | 0.067 52 | 22.77 | 2.18 | 14.1 |
| 11 | 0.1164 | 8.13 | 0.056 46 | 71.48 | 3.86 | 1.5 |
| 12 | 0.119 | 8.23 | 0.060 92 | 81.36 | 4.19 | 1.4 |
| 13 | 0.12 | 8.4 | 0.065 48 | 99.18 | 4.56 | 1.2 |
| 14 | 0.1294 | 9.07 | 0.0543 | 74.06 | 3.93 | 0.5 |
| 15 | 0.116 | 8.61 | 0.063 66 | 96.6 | 4.48 | 1.2 |
| 16 | 0.1192 | 8.65 | 0.057 36 | 78.57 | 4.04 | 0.7 |
| 17 | 0.205 | 1.84 | 0.1379 | 96.6 | 4.49 | 0.5 |
| 18 | 0.158 | 1.80 | 0.1301 | 84.04 | 4.19 | 1 |
| 19 | 0.161 | 1.88 | 0.1313 | 89.52 | 4.33 | 0.5 |
| 20 | 0.153 | 2.05 | 0.1218 | 83.88 | 4.19 | 0.2 |
| 21 | 0.138 | 4.35 | 0.9173 | 101.01 | 4.59 | 1.1 |
| 22 | 0.111 | 4.11 | 0.087 94 | 87.72 | 4.28 | 2 |
| 23 | 0.131 | 5.81 | 0.068 25 | 74.7 | 3.94 | 0.4 |

and 6(b). The critical value of d/T_w when γ_{tw} assumes a constant value depends on the temperature, that is, the critical values of d/T_w are 10, 15, and 20 at 600, 650, and 680 °C, respectively, and can be appreciated from Figs. 6(a) and 6(b).

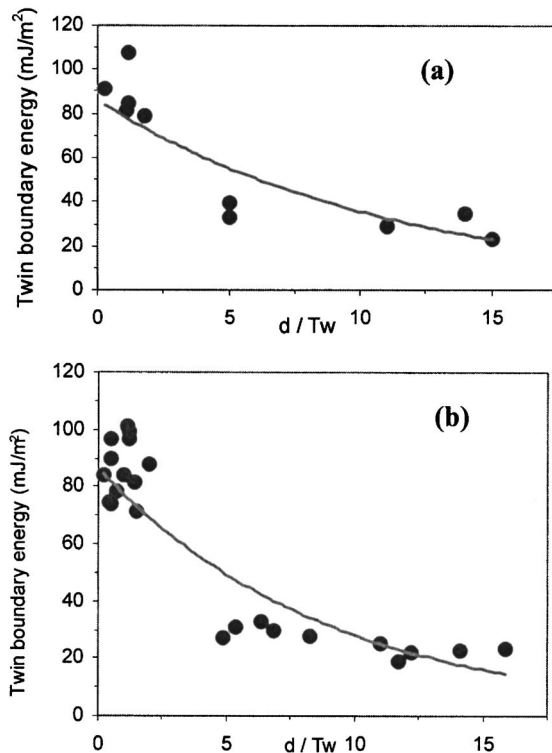


FIG. 6. Influence of d/T_w ratio on the twin energy determination by the tip method for different oxygenation temperatures, (a) 600 °C and (b) 650 °C.

B. Results from the twin tip method

Figure 7 is a plot of twin profile $h(x)$ vs $\sqrt{L^2 - x^2}$, where L is the half length of the twin and $L-x$ is the distance from the very tip for a twin in sample 450. Upon application of Eq. (7) and (9), the resulted value of $\gamma_{tw,450 \text{ °C}}$ is $75.7 \pm 10 \text{ mJ/m}^2$ and that of $M_{450 \text{ °C}}$ is $3.94 \times 10^4 \text{ N/m}^{3/2}$. Figure 8 is a similar plot of $h(x)$ vs $\sqrt{L^2 - x^2}$ for sample 500, with the corresponding $\gamma_{tw,500 \text{ °C}} = 52.6 \pm 13.7 \text{ mJ/m}^2$ and $M_{500 \text{ °C}} = 3.28 \times 10^4 \text{ N/m}^{3/2}$. Similar plots of $h(x)$ vs $\sqrt{L^2 - x^2}$ for twin tips in samples 600, 650, and 680 were graphed and the obtained twin boundary energies and the parameter M at 600, 650, and 680 °C are $\gamma_{tw,600 \text{ °C}}$

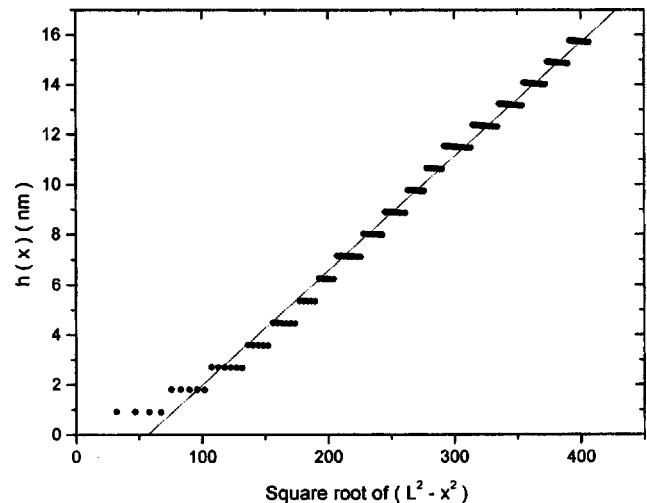


FIG. 7. A selected plot of twin thickness $h(x)$ vs the reduced coordinate $\sqrt{L^2 - x^2}$ for the twin tip region in sample 450.

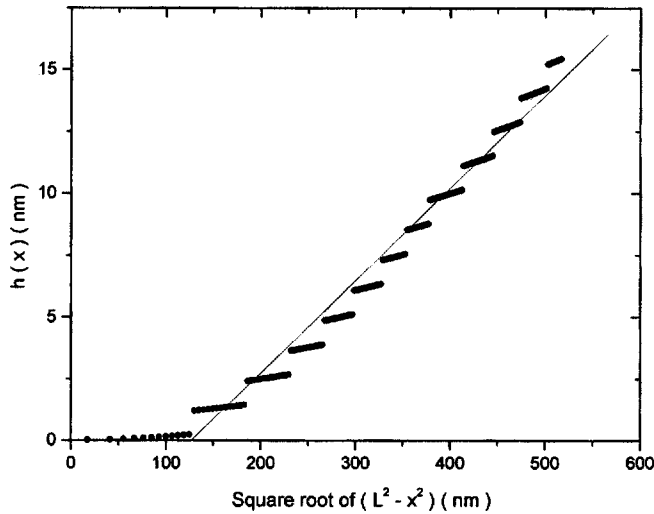


FIG. 8. A selected plot of twin thickness $h(x)$ vs the reduced coordinate $\sqrt{L^2 - x^2}$ for the twin tip region in sample 500.

$=29.5 \pm 6.6 \text{ mJ/m}^2$, $M_{600^\circ\text{C}} = 2.46 \times 10^4 \text{ N/m}^{3/2}$, $\gamma_{\text{tw},650^\circ\text{C}} = 22.6 \pm 2.1 \text{ mJ/m}^2$, $M_{650^\circ\text{C}} = 2.17 \times 10^4 \text{ N/m}^{3/2}$, $\gamma_{\text{tw},680^\circ\text{C}} = 17.5 \pm 1.9 \text{ mJ/m}^2$, $M_{680^\circ\text{C}} = 1.91 \times 10^4 \text{ N/m}^{3/2}$, respectively. All the results determined by the twin tip method are listed in the first three rows in Table V. The γ_{tw} 's and M 's of Y123 obtained by the twin tip method decrease with increasing temperature in the temperature range from 450 to 680 °C [see also Fig. 9(b)].

V. DISCUSSIONS

The scatter from the linear relation in the twin spacing versus $G^{1/2}$ as observed in Figs. 2 and 3 and the subsequent error range in γ_{tw} 's (Fig. 4) has to do with the assumptions inherent within the twin spacing method. First, the method is a two-dimensional (2D) approximation of a three-dimensional (3D) problem. Second, the method assumes equilibrium twin spacing established by a balance of twin boundary energy and strain energy. In reality, twinning is initiated by a critical shear stress in the (001) plane which is a stochastic process. Although local equilibrium is achieved among adjacent twins, true equilibrium between twin spacing and colony size may not get fully established.

The trend of the temperature dependence of the twin energy is the same as that for γ_{tw} obtained by the two methods (see second and fourth rows in Table V). However, the absolute γ_{tw} value at each temperature obtained by the tip method is much higher than that from the twin spacing method with α of 0.5. The twin boundary energies obtained by both methods should be the same. Within the twin spacing method, the geometric parameter α was taken as 0.5 when the twin tip angle was around 60–45 deg. As this angle is considerably smaller in the present samples, a larger α is justified. Accordingly, the geometrical factor α in the twin spacing method for each temperature is calculated such that the energies from both methods will be equal (fifth row). Since the variations of these α 's are within the error range, one cannot use them as an indication of true variation in strain volume. Yet the general strain volume is a lot larger than the first proposed. Therefore, an average α of 1.8 ± 0.33

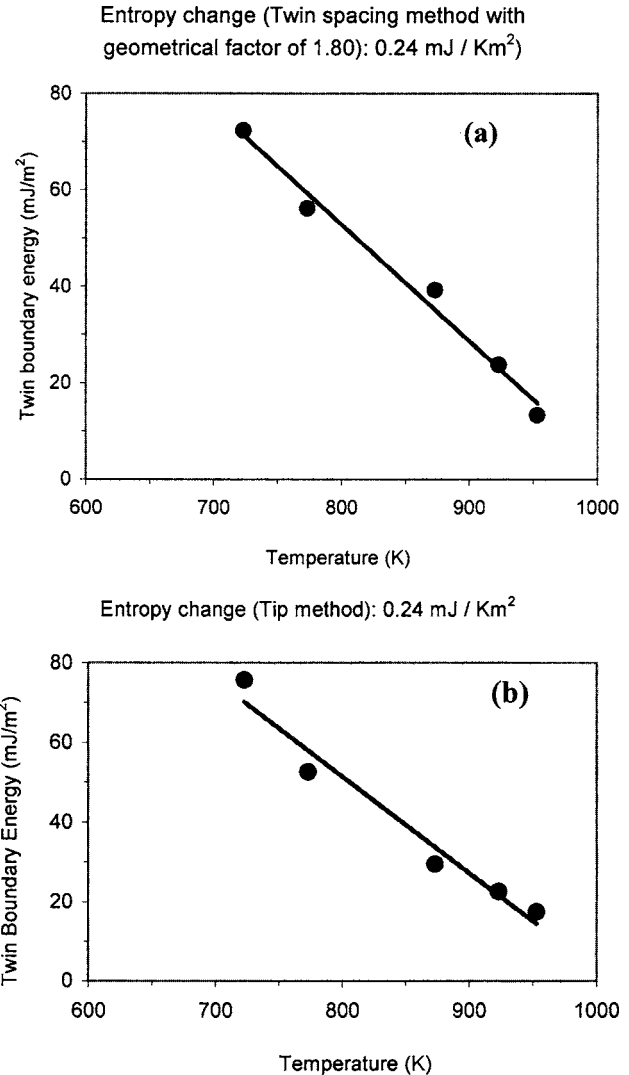


FIG. 9. Temperature dependence of the twin boundary energy obtained by the twin spacing method (a) and by the twin tip method (b). Slope corresponding to the entropy for twin boundary in MTG YBCO.

is determined and reapplied to the twin spacing method (see the last two rows in Table V). When the equation for the twin spacing method was first derived, the elastic strain volume was assumed to be confined to a twin length of T_w , then a choice of 0.5 for α was reasonable [as in Eq. (4)]. If the strained area of the twin tip is larger as associated with a more taper tip, a larger value for α is reasonable. The geometrical factor α can also be increased due to other contribution to the elastic strain energy term. In thin film of Y123, α is also reported to be higher because of the additional strain energy from the constraining substrate.²⁹

To determine whether present γ_{tw} values are reasonable, first, they are compared with the results by other researchers. As mentioned before, Boyko *et al.*⁹ calculated the twin boundary energy of YBCO by measuring the h/L ratio of wedged-shaped twins. There are mistakes in the paper: in the pileup dislocation model, a is the distance between the adjacent gliding planes of twin dislocations, and it is equal to $2.7 \times 10^{-10} \text{ m}$,²⁷ not $3.8 \times 10^{-10} \text{ m}$ of the lattice parameter a_0 along x axis. Also, the magnitude of Burgers vector \mathbf{b} of YBCO cannot be approximated to a , with actual $|\mathbf{b}| = 0.85$

TABLE V. Twin boundary energy of YBCO calculated by the twin tip method.

| Method | Sample | 450 | 500 | 600 | 650 | 680 |
|---------|---|-----------------|-----------------|-----------------|------------------|------------------|
| Tip | $M(10^4 \text{ N/m}^{3/2})$ | 3.94 ± 0.26 | 3.28 ± 0.42 | 2.46 ± 0.29 | 2.17 ± 0.1 | 1.91 ± 0.1 |
| | $\gamma_{\text{tw}}(\text{mJ/m}^2)$ | 75.7 ± 10.1 | 52.6 ± 13.7 | 29.5 ± 6.6 | 22.56 ± 2.13 | 17.47 ± 1.92 |
| | Error of γ_{tw} (%) | 13 | 26 | 22 | 9 | 11 |
| Spacing | $\gamma_{\text{tw}}(\text{mJ/m}^2)^a$ $\alpha=0.5$ | 20.1 ± 4.02 | 15.6 ± 3.12 | 10.9 ± 2.18 | 6.6 ± 1.32 | 3.7 ± 0.74 |
| | New α | 1.88 | 1.69 | 1.36 | 1.71 | 2.36 |
| | Average α | | | 1.80 ± 0.33 | | |
| | New $\gamma_{\text{tw}}(\text{mJ/m}^2)$ $\alpha=1.8$ | 72.36 | 56.16 | 39.24 | 23.76 | 13.32 |

^aTwin boundary energy calculated by spacing method with $\alpha=0.5$ (edge dislocation model).

$\times 10^{-11}$ m. If the above differences are corrected, the revised γ_{tw} is 27 mJ/m^2 , which is not unreasonable. They did not give oxygenation temperature. Yet, the revised result from their data is comparable to ours at 600–650 °C. The surface energies and twin boundary energies of several selected materials (H_2O , benzene, BaTiO_3 , Cu, Cr_2Ta , Cr_2Nb , Al, and Pd) (Table VI) are used to make a comparison with the twin boundary energy of Y123. The twin boundaries energies for the selected metals and alloys usually are several tens to 100 mJ/m^2 and even water has a surface energy of 73 mJ/m^2 . The earlier reported γ_{tw} 's of Y123 with value much lower than 10 mJ/m^2 seem unreal, while the present results are reasonable. Furthermore, the validity of the obtained twin boundary energy of Y123 can be roughly judged by the grain-boundary energy (about 5% of random high-angle grain-boundary energy).

Equipped with the twin boundary energies (γ_{tw} 's) at different temperatures, the enthalpy and entropy per unit area of twin boundaries in Y123 (i.e., Δh and Δs) can be evaluated from $\gamma_{\text{tw}}(T)$ which is the extra Gibbs free energy for twin boundaries per unit area (Δg). The governing relation is

$$\Delta g = \Delta h - T\Delta s, \quad (11)$$

where Δg is the Gibbs free energy, Δh is the enthalpy, and Δs is the entropy per unit twin boundary area. Both Δh and Δs are usually insensitive to temperature. Therefore, they can be determined by plotting γ_{tw} (i.e., Δg) versus temperature as shown in Figs. 9(a) and 9(b). The entropy for twin boundary per unit area (Δs) is 0.24 mJ/K m^2 from the slope. The enthalpy per unit boundary area (Δh) is 246 mJ/m^2 from the $T=0 \text{ K}$ intercept. Using those values, the twin boundary energy of Y123 at other temperatures can be obtained.

VI. CONCLUSIONS

The temperature-dependent twin boundary energy of Y123 has been determined by two different methods. They are the twin spacing method and twin shape method, while the geometrical factor α is in the twin spacing method is understood to be highly dependent on the tip shape and can be safely estimated. The twin boundary energy of Y123 decreases with increasing temperature. The premise of using a higher oxygenation temperature to generate finer twins for a higher critical current density and stronger flux-pinning force in melt-processed YBCO is theoretically sound. As the temperature increases from 450 to 680 °C the twin boundary energy decreases, which is consistent with a positive entropy. The γ_{tw} 's are calculated by the twin tip method: $\gamma_{\text{tw},450 \text{ °C}} = 75.7 \pm 10.1 \text{ mJ/m}^2$, $\gamma_{\text{tw},500 \text{ °C}} = 52.6 \pm 13.7 \text{ mJ/m}^2$, $\gamma_{\text{tw},600 \text{ °C}} = 29.5 \pm 6.6 \text{ mJ/m}^2$, $\gamma_{\text{tw},650 \text{ °C}} = 22.6 \pm 2.13 \text{ mJ/m}^2$, and $\gamma_{\text{tw},680 \text{ °C}} = 17.47 \pm 1.92 \text{ mJ/m}^2$. From 450 to 680 °C both the twin boundary energy γ_{tw} and the parameter M as determined by the twin tip method decrease with the increasing temperature, which is consistent with the results from the twin spacing method. Free twin tips are ideal for γ_{tw} determination by the twin tip method, and tips with the large enough distance from twin tip to the second twin variant (d) as compared to twin spacing (T_w), can be also used in giving accurate twin boundary energies. By comparing the twin energies obtained by twin spacing method and twin tip method, the geometrical factor α in twin spacing method is estimated to be 1.8 which better reflects the sharper twin tips. Ideally, the geometrical factor α can be independently evaluated by strain analyses of the twin tips. From the temperature dependence of twin boundary energy of Y123, per unit area energy (ΔS) and enthalpy (Δh) for twin boundaries are pro-

TABLE VI. Surface energies and twin boundary energies of selected materials.

| Material | H_2O | Benzene | BaTiO_3 | | Cu | Cr_2Ta | Cr_2Nb | Al | Pd |
|-------------------------------------|----------------------|---------|------------------|--------|---------------------|------------------------|------------------------|---|--------|
| | | | 90° domain | | | | | | |
| Temp. (°C) | 18 | 10 | 30 | NA | NA | NA | NA | NA | NA |
| $\gamma_{\text{tw}}(\text{mJ/m}^2)$ | 73.05 | 30.22 | 27.56 | 2–4, 3 | 45, 44 ^a | 33 ^b | 39 | 130 ± 15 , ^c 75 ^d | 97 ± 5 |
| Ref. | | 29 | 30 and 31 | 32 | 33 and 34 | 35 | 36 and 37 | 38 | |

^aAnnealed at 715 °C.

^bObtained by theoretical calculation.

^c{111}<112> twin systems.

^d(111) twins, experimental result.

TABLE VII. Comparison of reported γ_{tw} for Y123 with the parameter used and annealing temperatures. For the normalized γ_{tw} calculation (last column), the parameters used are $\alpha=1.8$, $\mu=C_{66}=95$ GPa and $\nu=0.3$. NA means not available from the references.

| γ_{tw} (mJ/m ²) | Parameters α, μ in GPa, ε | PtO ₂ | Temp. ^a (°C) | Method ^b | Ref. | Normalized γ_{tw} (mJ/m ²) |
|---------------------------------------|---|------------------|----------------------------|--------------------------|------------------------|--|
| 0.1 | 0.009 947, 100, 0.018 | No | NA | S | 3 | 41.8 ε : 0.016 |
| 1000 | NA, $E=143$ GPa, $\varepsilon=0.0167$ | No | NA | h/l ratio | 9 | 98.6 |
| 2.8 | 0.5, 59, 0.016 | No | NA | S | 4 | 23 |
| 8.5 | 0.5, 200, 0.016 | Yes | NA | S | 5 | 20.9 |
| 2.6 | 0.5, 200, 0.0145 | No | NA | S | 5 | 6.5 |
| 80 | 1.0, 200, NA | No | NA | S | 7 | 96.8 |
| <40 | 0.5, NA, 0.0165 | No | NA | S coercive stress 25 MPa | 8 | Upper limit of γ_{tw} |
| 46.53 | 0.32, 59, 0.0171 | No | 475 (SC) | S, S_{211} used | 10 | 103.9 |
| 18.28 | 0.32, 59, 0.0171 | Yes | 475 (SC) | S, S_{211} used | 10 | 40.8 |
| 20.1 | 0.5, 95, 0.0171, $\nu=0.3$ | Yes | 450 (I) | S | This work ^c | 72.4 |
| 15.6 | 0.5, 95, 0.0169, $\nu=0.3$ | Yes | 500 (I) | S | ... | 56.2 |
| 10.9 | 0.5, 95, 0.0165, $\nu=0.3$ | Yes | 600 (I) | S | ... | 39.2 |
| 6.6 | 0.5, 95, 0.0148, $\nu=0.3$ | Yes | 650 (I) | S | ... | 23.8 |
| 3.7 | 0.5, 95, 0.0148, $\nu=0.3$ | Yes | 680 (I) | S | ... | 13.3 |
| 75.7 | $C_{66}=95$, $\nu:0.3$ | Yes | 450 (I) | T | This work ^c | 75.7 |
| 52.6 | $C_{66}=95$, $\nu:0.3$ | Yes | 500 (I) | T | ... | 52.6 |
| 29.5 | $C_{66}=95$, $\nu:0.3$ | Yes | 600 (I) | T | ... | 29.5 |
| 22.56 | $C_{66}=95$, $\nu:0.3$ | Yes | 650 (I) | T | ... | 22.6 |
| 17.47 | $C_{66}=95$, $\nu:0.3$ | Yes | 680 (I) | T | ... | 17.5 |

^aI: Isothermal annealing; SC: Slow cooling annealing.

^bS: twin spacing method; T: twin tip method.

^cEdge dislocation model rather than screw dislocation model is used.

jected to be 0.24 mJ/K m² and 246 mJ/m², respectively. The twin boundary energy of YBCO at other temperatures can therefore be obtained. All the twin boundary energies of Y123 measured by both us and other researchers, normalized and original, are listed in Table VII for comparison.

ACKNOWLEDGMENTS

The authors thank Dr. V. S. Boyko and Dr. H. Ledbetter for discussions. This project and SWC's effort have been supported primarily by National Science Foundation.

¹M. Chopra, R. L. Meng, C. W. Chu, and S.-W. Chan, *J. Mater. Res.*, **11**, 1616 (1996).

²G. Arlt, D. Hennings, and G. de With, *J. Appl. Phys.* **58**, 1619 (1985).

³L. S. Chumbley, M. J. Kramer, M. R. Kim, and F. C. Laab, *Mater. Sci. Eng., A* **124**, L19 (1990).

⁴T. Roy and T. E. Mitchell, *Philos. Mag. A* **63**, 225 (1991).

⁵D. Muller and H. C. Freyhardt, *Philos. Mag. Lett.* **73**, 63 (1996).

⁶T. E. Mitchell and J. P. Hirth, *Acta Metall. Mater.* **39**, 1711 (1991).

⁷Y. Zhu, J. Taftø, and M. Suenaga, *MRS Bull.* **16**, 54 (1991).

⁸J. R. LaGraff and D. A. Payne, *Ferroelectrics* **130**, 87 (1992).

⁹Y. Boyko, H. Jaeger, M. Aslan, K. Schulze, and G. Petzow, *Mater. Lett.* **11**, 207 (1991).

¹⁰M. Chopra, S.-W. Chan, V. S. Boyko, R. L. Meng, and C. W. Chu, *The Proceeding of the 10th Anniversary High Temperature Superconductors Workshop*, Houston, Texas, March 1996, edited by B. Batlogg, C. W. Chu, W. K. Chu, D. U. Gubser, and K. A. Muller (World Scientific, Singapore, 1996), p. 175; S.-W. Chan, M. Chopra, V. S. Boyko, R. L. Meng, and C. W. Chu, in *The Proceeding of the 1997 International Workshop on Superconductivity (ISTEC)*, p. 311; M. Chopra, S.-W. Chan, V. S. Boyko, R. L. Meng, and C. W. Chu, "Twinning in Large Grains of YBa₂Cu₃O_{7-x}, as Affected by YBa₂Cu₃O₅ Particles," in preparation; M. Chopra and S.-W. Chan (unpublished).

¹¹P. Baumgart, S. Blumenroder, A. Erle, B. Hillebrands, P. Splittgerber, G. Guntherodt, and H. Schmidt, *Physica C* **162-164**, 1073 (1989).

¹²B. N. Lucas, W. C. Oliver, R. K. Williams, J. Brynstad, and M. E. O'Hern, *J. Mater. Res.* **6**, 2519 (1991).

¹³M. Lei and H. Ledbetter (unpublished).

¹⁴W. Reichardt, L. Pintschovius, B. Hennion, and F. Collin, *Supercond. Sci. Technol.* **1**, 173 (1988).

¹⁵H. Ledbetter and M. Lei, *J. Mater. Res.* **6**, 2253 (1991).

¹⁶M. Saint-Paul and J. Henry, *Solid State Commun.* **72**, 685 (1989).

¹⁷S. Suasmoro, D. S. Smith, M. Lejeune, M. Huger, and C. Gault, *J. Mater. Res.* **7**, 1629 (1992).

¹⁸M. Lei, J. L. Sarrao, W. M. Visscher, T. M. Bell, J. D. Thompson, A. Migliori, V. W. Welp, and B. W. Veal, *Phys. Rev. B* **47**, 6154 (1993).

¹⁹H. Ledbetter (private communication).

²⁰L. E. Murr, *Interfacial Phenomena* (Addison-Wesley, Reading, MA, 1975), p. 138.

²¹R. W. Cahn, *Physical Metallurgy*, 2nd ed. (North-Holland, Amsterdam, 1970), p. 1184.

²²C. Barrett and T. B. Massalski, *Structure of Metals*, 3rd ed. (Pergamon, New York, 1966), p. 413.

²³J. W. H. Tsai, S. Ling, J. C. Rodriguez, Z. Mustapha, and S.-W. Chan, *J. Electron. Mater.* **30**, 422 (2001).

²⁴Y. Zhu, M. Suenaga, and Y. Xu, *J. Mater. Res.* **5**, 1380 (1990).

²⁵V. S. Boyko, S.-W. Chan, and M. Chopra, *Phys. Rev. B* **63**, 224521 (2001); O. Jonprateep and S.-W. Chan, *IEEE Trans. Appl. Supercond.* **13**, 3502 (2003).

²⁶T. M. Shaw, S. L. Shinde, D. Dimos, R. F. Cook, P. R. Duncombe, and C. Kroll, *J. Mater. Res.* **4**, 248 (1989).

²⁷Y. Zhu, and M. Suenaga, *Philos. Mag. A* **66**, 47 (1992).

²⁸Program NXSCAN from Incorporated Research Institutions for Seismology (IRIS).

²⁹S. K. Streiffer, E. M. Zielinski, B. M. Lairson, and J. C. Bravman, *Appl. Phys. Lett.* **58**, 2171 (1991).

³⁰R. C. Weast, *CRC Handbook of Chemistry and Physics*, 49th ed. (CRC, Cleveland, OH, 1968).

³¹M. E. Lines and A. M. Glass, *Principles and Applications of Ferroelectrics and Related Materials* (Clarendon, Oxford, 1977).

³²R. E. Reed-Hill, *Physical Metallurgy Principles*, 2nd ed. (Wadsworth, Monterey, CA, 1973).

³³C. Valenzuela, *Trans. Metall. Soc. AIME* **233**, 1911 (1965).

³⁴R. L. Fullman, *J. Appl. Phys.* **22**, 448 (1951).

³⁵S. Hong, C. L. Fu, and M. H. Yoo, *Intermetallics* **7**, 1169 (1999).

³⁶S. Hong, C. L. Fu, and M. H. Yoo, *Philos. Mag. A* **80**, 871 (2000).

³⁷J.-H. Xu, W. Lin, and A. J. Freeman, *Phys. Rev. B* **43**, 2018 (1991).

³⁸J. P. Hirth and J. Lothe, *Theory of Dislocations*, 2nd ed. (Wiley, New York, 1982), p. 306.